

# Piezoelectric properties of II–IV/I–V and II–IV/III–III ferroelectric perovskite superlattices

Alexander I. Lebedev\*

*Physics Department, Moscow State University, 119991 Moscow, Russia*

(Dated: September 3, 2021)

The stability of high-symmetry  $P4mm$  polar phase in eleven ferroelectric perovskite superlattices with the polar discontinuity is studied from first principles. In most superlattices, this phase exhibits either the ferroelectric or the antiferrodistortive instability, or both of them. The structure of the ground state and, for a number of systems, also of metastable phases in these superlattices is found. The spontaneous polarization and piezoelectric properties of superlattices are calculated. The appearance of high piezoelectric coefficients (up to 150–270 pC/N) in some superlattices is associated with the strain-induced local rearrangement of certain atomic groups in the primitive cell.

**Ferroelectrics** 567, 89 (2020); DOI: 10.1080/00150193.2020.1791592

Keywords: Ferroelectric superlattices; polar discontinuity; first-principles calculations; piezoelectricity; perovskites

## I. INTRODUCTION

In recent years, much attention has been paid to studies of low-dimensional structures in which new physical phenomena that have no analogues in bulk materials have been discovered. Due to these new functionalities, these materials are considered as very promising for future applications in electronics. Ferroelectric superlattices (SL)—quasi-two-dimensional structures with artificial periodicity whose properties can be easily tuned to obtain necessary functionality—belong to this interesting class of materials.

Most of the previous studies of ferroelectric perovskite superlattices were carried out on II–IV/II–IV or I–V/I–V type superlattices (here, the numbers indicate the valence of atoms that enter the  $A$  and  $B$  sites of the  $ABO_3$  perovskite structure). In such SLs, there are no double electric layers at the interface between two dielectric materials, and therefore, they are macroscopically electrically neutral both in the bulk and at the interface (see [1–10] and references therein).

Studies of the  $SrTiO_3/LaAlO_3$  heterostructures have revealed new interesting phenomena that appear in these structures as a result of the so-called polar discontinuity—of a polarization jump produced by a violation in the sequence of charged layers at the interface between II–IV and III–III materials. These effects include the appearance of a conducting layer near the interface (a two-dimensional electron gas), its magnetism, and even superconductivity [11–13]. These phenomena can be controlled using an external electric field [14]. The divergence of the electrostatic potential in such heterostructures, which results in the appearance of conducting layers at the interface between two dielectrics, was called a polar catastrophe. The possibility of the appearance of the two-dimensional electron gas at the

interface between a ferroelectric and a nonpolar dielectric in perovskites was systematically studied in Ref. [15]. Later it was realized that conducting layers can also be obtained in ferroelectric structures without the polar discontinuity [16]. This made it possible to create new types of electronic devices—ferroelectric structures with switchable giant tunneling electroresistance [17, 18], whose idea is based on earlier works [19, 20]. We note that the appearance of similar phenomena can be expected in epitaxial films of II–IV perovskites grown on  $DyScO_3$ ,  $GdScO_3$ ,  $NdScO_3$ , and  $NdGaO_3$  substrates, in which a polar discontinuity at the interface is possible.

Until now, theoretical studies of superlattices with the polar discontinuity have focused on the study of the polarization and electric field distributions in these structures and on the search for conditions of the appearance of a two-dimensional electron gas at the interface [21–27]. The questions about the stability of the high-symmetry structure in such SLs, the possibility of phase transitions in them, and the physical properties of possible low-symmetry phases were not analyzed. At the same time, the ferroelectric and antiferrodistortive (AFD) instabilities characteristic of many perovskites can lead to strong distortions of the structure of SLs, and the earlier predictions of physical properties obtained without taking these distortions into account may be incorrect.

One of the questions that have not been studied in detail earlier is the question about the piezoelectric properties of superlattices with the polar discontinuity. The calculations of the properties of such SLs were limited to the calculations of them in the high-symmetry  $P4mm$  phase [28, 29]. It is known that the record-high piezoelectric coefficients in  $PbTiO_3$ -based solid solutions near the morphotropic boundary [30] are associated with the ease of inclination of the polarization vector from the [100] direction to the [111] direction under the influence of an electric field [31]. The polar discontinuity in superlattices enables, under certain conditions, to create high values of irreversible polarization in their structures. That is why it seemed interesting to check whether it is possible to

---

\* swan@scon155.phys.msu.ru

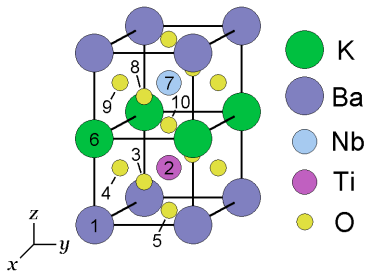


FIG. 1. The superlattice geometry.

obtain high piezoelectric coefficients in superlattices with the polar discontinuity using the strain-induced inclination of the polarization vector. In Ref. [28], superlattices with the polar discontinuity were already considered as a way to obtain stable, weakly temperature-dependent piezoelectric properties.

## II. CALCULATION TECHNIQUE

In this work, the properties of eleven free-standing [001]-oriented short-period II-IV/I-V and II-IV/III-III superlattices with the polar discontinuity and a thickness of individual layers of one unit cell are studied using first-principles calculations. The geometry of the superlattices is shown in Fig. 1. The choice of free-standing superlattices is due to the fact that for any short-period superlattice grown on a substrate, mismatch dislocations and other defects appear in the transition layer with a typical thickness of  $\sim 100$  Å because of a mismatch between the equilibrium in-plane lattice parameter of the superlattice and that of the substrate. As a result, the in-plane lattice parameter of the superlattice relaxes to that of the free-standing superlattice. This is why in most thick experimentally grown SLs, the in-plane lattice parameter is close to that of a free-standing SL.

The first-principles calculations were performed within the density functional theory using the ABINIT program and norm-conserving pseudopotentials constructed according to the RRKJ scheme [32] in the local density approximation (LDA), like in Ref. [33]. The cutoff energy was 30 Ha (816 eV) except for Ta-containing systems, in which it was 40 Ha (1088 eV). Integration over the Brillouin zone was carried out using a  $8 \times 8 \times 4$  Monkhorst-Pack mesh for the high-symmetry structure and meshes with equivalent density of  $\mathbf{k}$ -points for the low-symmetry phases. The equilibrium lattice parameters and atomic positions were calculated by relaxing forces acting on the atoms to values less than  $2 \cdot 10^{-6}$  Ha/Bohr ( $0.1$  meV/Å). The phonon spectra, the tensor of piezoelectric stress coefficients  $e_{i\mu}$ , and the elastic compliance tensor  $S_{\mu\nu}$  were calculated using the density-functional perturbation theory. The  $e_{i\mu}$  values were then converted to piezoelectric strain coefficients  $d_{i\nu}$  using the formula  $d_{i\nu} = e_{i\mu} S_{\mu\nu}$ , and for monoclinic cells the tensor components were trans-

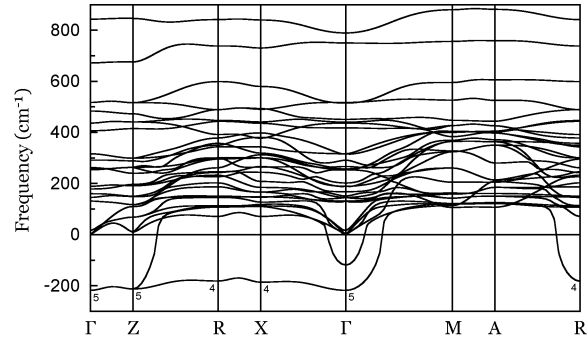


FIG. 2. The phonon spectrum of the  $\text{KNbO}_3/\text{BaTiO}_3$  superlattice in the  $P4mm$  phase. The numbers near the curves indicate the symmetry of unstable modes.

formed to the standard setting of the monoclinic cell, in which the polarization vector lies in the  $xz$  plane.

## III. RESULTS AND DISCUSSION

To begin with, it should be noted that the electrical conductivity is usually a factor that prevents many applications of the ferroelectric properties. Since the experiments on structures with the polar discontinuity often revealed metallic conductivity at the interface, it was necessary to make sure that the superlattices under study are insulating. The calculations confirmed that in all superlattices studied in this work, the conduction band is separated from the valence band by a sufficiently large energy gap, and so all studied SLs are dielectrics.

Since the layer sequence in considered superlattices does not admit the reversal of  $z \rightarrow -z$  (Fig. 1), the superlattices are always polar and their high-symmetry phase has the  $P4mm$  symmetry. However, this structure can exhibit various instabilities characteristic of crystals with the perovskite structure: either the ferroelectric instability, or the antiferrodistortive one, or both of them simultaneously. The ground state of superlattices was searched in the traditional way [5, 6]: first, the structures resulting from the condensation of all unstable phonons found in the phonon spectrum of the  $P4mm$  phase were calculated, taking into account their possible degeneracy. Then, by calculating the phonon spectra at all high-symmetry points of the Brillouin zone and the elastic tensor of these structures, the stability of the obtained solutions was checked. In the case when an instability in any of these structures was found, the search for the ground state was continued until a structure whose phonon spectrum has no unstable modes and the positive definite matrix composed of the elastic tensor components in the Voigt notation is found. In this case, the conclusion that a stable phase which may be a ground state can be made. The problem here is in that in chains

of phases generated by different octahedra rotations, several stable states can be found, as was shown recently for  $\text{SrTiO}_3$  [34]. In this case, the ground state is the stable phase with the lowest total energy, and other stable phases should be considered as metastable. If the energy of such metastable solutions differs little from the energy of the ground state, they should be considered as solutions that can be observed in experiment, and for them, as well as for the ground state, an analysis of their physical properties should also be carried out.

Calculations of the phonon spectra showed that in most studied SLs (except for  $\text{BaTiO}_3/\text{LaAlO}_3$ ,  $\text{SrTiO}_3/\text{LaAlO}_3$ ,  $\text{PbTiO}_3/\text{KTaO}_3$ , and  $\text{PbTiO}_3/\text{LaAlO}_3$ ), the high-symmetry  $P4mm$  phase exhibits the ferroelectric instability with respect to the in-plane distortion of the structure or, in other words, with respect to the inclination of the polarization vector. The phonon spectrum of a such superlattice,  $\text{KNbO}_3/\text{BaTiO}_3$ , is shown in Fig. 2. It can be seen that in addition to the instability at the  $\Gamma$  point, the instabilities also appear at the  $X$ ,  $R$ , and  $Z$  points of the Brillouin zone. We have already encountered a similar situation in  $\text{KNbO}_3/\text{KTaO}_3$  [7] and  $\text{BaTiO}_3/\text{BaZrO}_3$  [9] SLs.

An instability zone, which is observed as a band of imaginary phonon frequencies on the  $\Gamma$ - $Z$ - $R$ - $X$ - $\Gamma$  line (imaginary frequencies are represented in the figure by negative numbers), is a consequence of the ferroelectric instability in  $\dots\text{-Ti-O-}\dots$  chains propagating in the plane of SL—the so-called chain instability [35]. Indeed, an analysis of phonon eigenvectors of these modes shows that at all above-mentioned points of the Brillouin zone, the out-of-phase, transverse,  $xy$ -polarized displacements of Ti and O atoms in chains propagating in the  $[100]$  and  $[010]$  directions dominate in the vibrations. In superlattices based on  $\text{BaTiO}_3$  and  $\text{SrTiO}_3$ , the displacements of the Nb(Ta) atoms were small, whereas in superlattices based on  $\text{SrZrO}_3$  and  $\text{BaZrO}_3$ , as well as in the  $\text{PbTiO}_3/\text{KNbO}_3$  SL, the chain instability appears mainly in  $\dots\text{-Nb-O-}\dots$  chains. At the center of the Brillouin zone, the described displacements pattern corresponds to a doubly degenerate ferroelectric  $E$  mode ( $\Gamma_5$ ).[36]

Of two possible polar phases resulting from the condensation of the unstable  $E$  mode, the  $Cm$  phase with atomic displacements along the  $[110]$  direction was the lowest-energy phase for all superlattices. The displacements in the  $[100]$  direction were energetically less favorable, which is apparently due to a tendency of bulk  $\text{BaTiO}_3$  and  $\text{KNbO}_3$  to polarize along the  $[111]$  direction in the ground state. As an example, the energies of different low-symmetry phases for the  $\text{KNbO}_3/\text{BaTiO}_3$  SL are given in Table I. The structures obtained from the condensation of  $Z_5$ ,  $R_4$ , and  $X_4$  phonons had a higher energy as compared to that of the  $Cm$  phase.

The absence of the ferroelectric instability in the  $P4mm$  phase of  $\text{PbTiO}_3/\text{KTaO}_3$  and  $\text{PbTiO}_3/\text{LaAlO}_3$  superlattices can be explained by a tendency of bulk  $\text{PbTiO}_3$  to polarize along the  $[001]$  axis. This instability

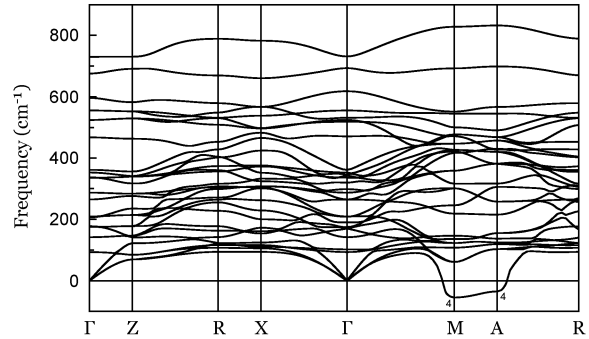


FIG. 3. The phonon spectrum of the  $\text{BaTiO}_3/\text{LaAlO}_3$  superlattice in the  $P4mm$  phase. The numbers near the curves indicate the symmetry of unstable modes.

was also absent in the  $\text{SrTiO}_3/\text{LaAlO}_3$  SL, in which both constituents are nonpolar. In addition, the ferroelectric instability did not appear in the  $\text{BaTiO}_3/\text{LaAlO}_3$  superlattice, in which its absence is a consequence of the strong (by 2.3%) in-plane compression of  $\text{BaTiO}_3$  layers. Our calculations of the effect of strain on the ground-state structure of  $\text{BaTiO}_3$  showed that the biaxial compression of 1% is sufficient to change the most stable polar phase in it to the  $P4mm$  phase, in agreement with [37, 38].

Along with the ferroelectric instability, in the high-symmetry  $P4mm$  phase of a number of superlattices ( $\text{KNbO}_3/\text{SrTiO}_3$ ,  $\text{KNbO}_3/\text{SrZrO}_3$ ,  $\text{BaTiO}_3/\text{LaAlO}_3$ ,  $\text{SrTiO}_3/\text{KTaO}_3$ ,  $\text{SrTiO}_3/\text{LaAlO}_3$ , and  $\text{PbTiO}_3/\text{LaAlO}_3$ ) an AFD instability with the octahedra rotations around the  $z$  axis is observed. It can be clearly seen by the appearance of unstable phonons on the  $M$ - $A$  line (Fig. 3). The occurrence of the AFD instability in SLs clearly correlates with the existence of this instability in one or both of the constituent materials ( $\text{SrTiO}_3$ ,  $\text{SrZrO}_3$ ,  $\text{LaAlO}_3$ ). A comparison of the energies of phases resulting from the condensation of phonons at the  $M$  and  $A$  points of the Brillouin zone shows that of two phases resulting from the  $M_4$  phonon condensation (space group  $P4bm$ ) and from the  $A_4$  phonon condensation (space group  $I4cm$ ), the  $P4bm$  phase was always more energetically favorable. However, since the energy difference between these phases is small, and each of them can exhibit the ferroelectric instability, it was necessary to consider all polar subgroups of these phases when searching for the ground state.

The calculations showed that the ferroelectric instability of the  $P4bm$  and  $I4cm$  phases is characteristic of  $\text{KNbO}_3/\text{SrTiO}_3$ ,  $\text{SrTiO}_3/\text{KTaO}_3$ , and  $\text{KNbO}_3/\text{SrZrO}_3$  SLs. Of two structures,  $Cm$  and  $Pc$ , into which the  $P4bm$  structure can transform upon polar distortion, the  $Pc$  phase with the polarization along the  $[110]$  direction of the pseudocubic cell always had a lower energy. For a random starting polar displacement from the  $I4cm$  phase, the structure always relaxed to the  $Cc$  phase, in

TABLE I. The energies (in meV per 10-atom supercell) of different low-symmetry phases resulting from condensation of unstable phonons at different points of the Brillouin zone for  $\text{KNbO}_3/\text{BaTiO}_3$  and  $\text{KNbO}_3/\text{SrZrO}_3$  short-period superlattices.

Phase	Unstable phonon	Energy	Phase	Unstable phonon	Energy
$\text{KNbO}_3/\text{BaTiO}_3$ superlattice					
$P4mm$	—	0	$Pm$	$\Gamma_5(\eta, 0)$	-27.8
$Abm2$	$R_4$	-13.8	$Cmc2_1$	$Z_5(\eta, \eta)$	-31.0
$Pma2$	$X_4$	-14.8	$Cm$	$\Gamma_5(\eta, \eta)$	-38.6
$Pmc2_1$	$Z_5(\eta, 0)$	-21.3			
$\text{KNbO}_3/\text{SrZrO}_3$ superlattice					
$P4mm$	—	0	$Pc$	$Z_5(\eta, 0) + \Gamma_5(0, \xi)$	-19.2
$I4cm$	$A_4$	-1.3	$Pma2$	$M_5(\eta, 0)$	-19.9
$P4bm$	$M_4$	-2.1	$Cm$	$\Gamma_5(\eta, \eta)$	-20.0
$Abm2$	$R_4$	-4.7	$P2$	$X_3 + X_4$	-20.7
$Pma2$	$X_4$	-6.7	$Cc$	$A_4 + \Gamma_5(\eta, \eta)$	-24.1
$Pmm2$	$X_3$	-12.4	$Pm$	$X_3 + \Gamma_5(0, \eta)$	-24.9
$Pmc2_1$	$Z_5(\eta, 0)$	-12.9	$Cmm2$	$M_5(\eta, \eta)$	-26.9
$Pm$	$\Gamma_5(\eta, 0)$	-13.7	$Pm$	$X_3 + \Gamma_5(\eta, 0)$	-27.6
$Pc$	$R_4 + \Gamma_5(\eta, 0)$	-15.4	$Pm$	$M_5(\eta, 0) + \Gamma_5(\xi, \xi)$	-36.9
$Pc$	$X_4 + \Gamma_5(\eta, 0)$	-17.0	$Cm$	$M_4 + \Gamma_5(\eta, 0)$	-39.4
$Cmc2_1$	$Z_5(\eta, \eta)$	-18.9	$Pc$	$M_4 + \Gamma_5(\eta, \eta)$	-51.9

which the polarization is also directed along the [110] direction of the pseudocubic cell. For first two superlattices, the energy difference between the  $Cc$  and  $Pc$  phases was only 0.5–0.7 meV. Taking into account that the analysis proved the stability of both phases, the  $Cc$  phase should be considered as metastable. As the energy difference between the two phases is very small, there is a real possibility that both structures can occur in the experiment simultaneously. That is why the properties of these superlattices were calculated below for both the  $Pc$  and  $Cc$  phases.

The most complex picture was observed in superlattices, in which both ferroelectric and AFD instabilities were simultaneously present. An example of such a system is the  $\text{KNbO}_3/\text{SrZrO}_3$  SL. The energies of different phases for this superlattice are given in Table I.

In addition to the above-discussed unstable  $M_4$  mode, one more doubly degenerate unstable  $M_5$  mode was observed in the phonon spectra of the  $P4mm$  phase of four SLs ( $\text{KNbO}_3/\text{SrTiO}_3$ ,  $\text{KNbO}_3/\text{SrZrO}_3$ ,  $\text{SrTiO}_3/\text{LaAlO}_3$ , and  $\text{PbTiO}_3/\text{LaAlO}_3$ ). This mode describes the rotations of the octahedra around one or both of the  $x$  and  $y$  axes. The distortions described by this mode with the  $(\eta, 0)$  and  $(\eta, \eta)$  order parameters resulted in the  $Pma2$  and  $Cmm2$  phases, of which the  $Cmm2$  phase always had a lower energy. Both these phases are characterized by the ferroelectric instability. An analysis of the polar subgroups of the  $Pma2$  and  $Cmm2$  phases in  $\text{KNbO}_3/\text{SrTiO}_3$  and  $\text{KNbO}_3/\text{SrZrO}_3$  SLs showed that among them the  $Pc$  phase, which is already familiar to us, has the lowest energy. It may seem strange that the same  $Pc$  phase appears as a result of condensation of phonons described by two different irreducible represen-

tations ( $M_4$  and  $M_5$ ). However, it should be taken into account that the vertical axis of the octahedra in the  $Pc$  phase is slightly inclined, that is, in reality this phase is described by two nonzero rotations around the coordinate axes. This explains why two structures, in which the distortions are described by different irreducible representations, relax to the same  $Pc$  phase when the polar displacements are switched on. In  $\text{SrTiO}_3/\text{LaAlO}_3$  and  $\text{PbTiO}_3/\text{LaAlO}_3$  SLs, both  $Pma2$  and  $Cmm2$  structures relax to the “nonpolar”  $P4bm$  phase when the polar displacements are switched on.

The space groups of the energetically most favorable phases obtained for all studied SLs are given in Table II. It is seen that in superlattices exhibiting only the ferroelectric instability, the  $Cm$  phase is the ground state. In SLs exhibiting only the AFD instability, the  $P4bm$  phase is the ground state. And, finally, in superlattices in which both instabilities are present in the  $P4mm$  phase, the  $Pc$  phase is the ground state. The difference between our results and the results of earlier calculations for the  $\text{KNbO}_3/\text{BaTiO}_3$  SL [27] is due to the fact that the calculations [27] were performed for the superlattice clamped on the  $\text{SrTiO}_3$  substrate: in such SL, the  $P4mm$  phase is indeed the ground state.

The energy gain  $\Delta E$  per 10-atom formula unit, which results from the ferroelectric distortion, is also given in Table II. The obtained values show that at room temperature, the predicted ground-state structures are likely to be observed for  $\text{KNbO}_3/\text{BaTiO}_3$ ,  $\text{KNbO}_3/\text{BaZrO}_3$ , and  $\text{KNbO}_3/\text{SrZrO}_3$  SLs. For the ground-state structures of all superlattices, the spontaneous polarization and the piezoelectric tensor will be calculated below.

Classical electrostatics of an electrically neutral inter-

TABLE II. Calculated polarization and the energy gain upon the ferroelectric distortion for all studied short-period superlattices with the polar discontinuity. The polarization values are in  $\text{C}/\text{m}^2$ , the energy values are in  $\text{meV}$ .

Superlattice	Space group	$P_x$	$P_y$	$P_z$	$\Delta E$
$\text{KNbO}_3/\text{PbTiO}_3$	$Cm$	0.181	0	0.567	3.34
$\text{KNbO}_3/\text{BaTiO}_3$	$Cm$	0.338	0	-0.033	38.61
$\text{KNbO}_3/\text{BaZrO}_3$	$Cm$	0.229	0	0.181	33.82
$\text{KNbO}_3/\text{SrTiO}_3$	$Pc$	0.281	0	0.066	53.31; 8.96 <sup>a</sup>
$\text{KNbO}_3/\text{SrZrO}_3$	$Pc$	0.268	0	0.187	51.86; 49.80 <sup>a</sup>
$\text{BaTiO}_3/\text{KTaO}_3$	$Cm$	0.180	0	0.130	9.73
$\text{BaTiO}_3/\text{LaAlO}_3$	$P4bm$	0	0	0.057	—
$\text{SrTiO}_3/\text{KTaO}_3$	$Pc$	0.105	0	0.141	11.86; 0.82 <sup>a</sup>
$\text{SrTiO}_3/\text{LaAlO}_3$	$P4bm$	0	0	0.012	—
$\text{PbTiO}_3/\text{KTaO}_3$	$P4mm$	0	0	0.454	—
$\text{PbTiO}_3/\text{LaAlO}_3$	$P4bm$	0	0	0.119	—

<sup>a</sup> The energies relative to that of the “nonpolar”  $P4bm$  phase.

face between two dielectrics requires that the components of the electric displacement field normal to this interface are equal in two materials. If the materials have different spontaneous polarizations, then a bound electric charge appears at the interface, and the electric field generated by it makes the electric displacement fields equal in two materials.

In superlattices with the polar discontinuity, the violation of the order of charged  $AO$  and  $BO_2$  planes generates an additional electrostatic perturbation at the interfaces and creates a polarization jump of  $\Delta P = e/2a^2$  at every interface in the superlattices (here  $a$  is the in-plane lattice parameter of the SL) [21]. An elegant solution to this problem, which can be used in the general case, was proposed in [25] within the framework of the modern theory of polarization (the Berry phase formalism). An application of this approach to our superlattices enabled us to calculate the electric displacement field in them and to use it to determine an average polarization of SLs. In this work, we are interested precisely in this quantity. The polarization values in individual layers can be calculated by correcting the obtained average polarization taking into account the jump in the ionic contribution to the Berry phase at the interface and dielectric constants of individual constituents.[39]

When calculating the polarization by the Berry phase method, it should be borne in mind that the ionic contributions to the Berry phase are different in nonpolar  $Pm\bar{3}m$  phases of II–IV and I–V perovskites. This is why for each SL with the polar discontinuity it is necessary first to find the Berry phase of a nonpolar structure before calculating the polarization. Unfortunately, in our case the determination of the  $z$  component of the Berry phase is a problem because in the high-symmetry  $P4mm$  phase, which does not have a mirror plane  $\sigma_z$ , it is impossible to reverse the polarization or to construct a nonpolar structure. To estimate  $P_z$ , we considered unrelaxed structures with ideal atomic positions corresponding to

the cubic perovskite structure in both layers. In this structure, the electron contribution to the Berry phase is nonzero because of the redistribution of the electron density between the layers, and the ionic contribution reflects the difference in the Berry phases of individual perovskites. The change of the Berry phase upon the transition from the described unrelaxed structure to the ground-state structure was used to calculate the average polarization using the standard formula. To correctly determine the polarization from the change of the Berry phase, which is determined with an accuracy of  $2\pi m$ , for all SLs the calculations were also performed for one intermediate point at which the atoms are located halfway between the unrelaxed structure and the ground state.

The calculated polarizations are given in Table II. The components of the polarization vector are given relative to the axes of standard crystallographic settings for tetragonal and monoclinic cells (their axes are rotated in the  $xy$  plane by  $45^\circ$  relative to each other). The comparison of polarizations calculated in structures with and without octahedral rotations shows that in structures with the  $Pc$  space group, the neglect of the AFD rotations can lead to an error in determining  $P_z$  up to 30% and, in some cases, even to an error in the sign of this quantity. For the  $P4mm$  phases, the obtained values agree well with the published values of  $P_z = 0.532 \text{ C}/\text{m}^2$  for the  $\text{PbTiO}_3/\text{KNbO}_3$  SL and  $P_z = 0.202 \text{ C}/\text{m}^2$  for the  $\text{PbTiO}_3/\text{LaAlO}_3$  SL [29], and with the  $P_z = 0.38 \text{ C}/\text{m}^2$  value for the  $\text{PbTiO}_3/\text{KTaO}_3$  SL [40].

The reason for our interest to the ferroelectric instability in superlattices with the polar discontinuity is that in such SLs it is possible to obtain sufficiently high piezoelectric coefficients associated with the ferroelectric phase transitions occurring in them. The literature data on the piezoelectric properties of such superlattices are limited to calculations for the  $P4mm$  phases of  $\text{PbTiO}_3/\text{LaAlO}_3$  and  $\text{KNbO}_3/\text{PbTiO}_3$  SLs [28, 29] and of the  $\text{PbTiO}_3/\text{KTaO}_3$  one [40]. As the ground-

TABLE III. Nonzero components of the piezoelectric tensor  $d_{i\nu}$  (in pC/N) in the ground state of all studied short-period superlattices with the polar discontinuity.

Superlattice	$d_{11}$	$d_{12}$	$d_{13}$	$d_{15}$	$d_{24}$	$d_{26}$	$d_{31}$	$d_{32}$	$d_{33}$	$d_{35}$
KNbO <sub>3</sub> /PbTiO <sub>3</sub>	13.4	3.7	-13.9	158.3	273.3	137.3	-3.0	-2.9	-10.9	-0.8
KNbO <sub>3</sub> /BaTiO <sub>3</sub>	23.5	9.6	-12.7	3.8	-2.8	106.4	10.7	7.9	-16.3	17.4
KNbO <sub>3</sub> /BaZrO <sub>3</sub>	16.3	4.7	-11.7	5.6	7.9	20.8	-8.9	-7.3	16.7	1.8
KNbO <sub>3</sub> /SrTiO <sub>3</sub>	35.9	15.3	-19.1	8.3	41.7	151.0	-22.0	-12.1	16.1	9.4
KNbO <sub>3</sub> /SrZrO <sub>3</sub>	30.8	10.1	-18.8	9.1	11.0	85.5	-18.1	-9.8	17.7	12.9
BaTiO <sub>3</sub> /KTaO <sub>3</sub>	19.2	9.5	-18.5	2.5	7.9	25.3	-18.1	-11.6	43.4	10.1
BaTiO <sub>3</sub> /LaAlO <sub>3</sub>	—	—	—	1.4	1.4	—	3.0	3.0	-4.6	—
SrTiO <sub>3</sub> /KTaO <sub>3</sub>	39.7	22.8	-27.6	28.2	46.9	41.2	-18.4	-13.0	26.1	-4.2
SrTiO <sub>3</sub> /LaAlO <sub>3</sub>	—	—	—	2.0	2.0	—	1.0	1.0	-1.6	—
PbTiO <sub>3</sub> /KTaO <sub>3</sub>	—	—	—	91.4	91.4	—	-8.8	-8.8	41.2	—
PbTiO <sub>3</sub> /LaAlO <sub>3</sub>	—	—	—	158.6	158.6	—	-4.3	-4.3	-2.8	—

state structure in the first two superlattices differs from  $P4mm$ , there is a need for more correct calculations for these superlattices. For other SLs considered in this work, no data on their piezoelectric properties exist.

In SLs with a tetragonal ground-state structure, in which the polarization is directed along the  $z$  axis, five components of the piezoelectric tensor are nonzero. Among them, the highest values of  $d_{i\nu}$  were obtained for PbTiO<sub>3</sub>/KTaO<sub>3</sub> and PbTiO<sub>3</sub>/LaAlO<sub>3</sub> SLs (Table III). Interestingly, among these coefficients, the  $d_{15}$  values turned out to be the largest. This coefficient characterizes the polarization  $P_x$  that appears as a result of the  $xz$  shear strain of the unit cell, that is, as a result of inclination of the polarization vector. However, no clear correlation between  $d_{15}$  and  $P_z$  values was observed. Moreover, in the related system, BaTiO<sub>3</sub>/LaAlO<sub>3</sub>, the piezoelectric coefficients were very small (Table III). This means that the inclination of the polarization vector as a way of obtaining high values of piezoelectric coefficients is not effective.

In SLs with a monoclinic ground-state structure, in which the polarization vector lies in the  $xz$  plane, the piezoelectric tensor is characterized by ten nonzero components. In these structures, the highest values of  $d_{i\nu}$  were the  $d_{24}$  and  $d_{26}$  coefficients, which describe the appearance of polarization in the  $y$  direction normal to the  $xz$  plane under the  $yz$  and  $xy$  shear strain. An analysis of the obtained data also does not find a clear correlation between the piezoelectric coefficients and the average polarization in these structures. The stretching of the unit cell in the  $xz$  plane does result in a change in polarization, but the corresponding piezoelectric coefficients ( $d_{11}$  and  $d_{33}$ , see Table III) are not the largest.

To understand the mechanism of the appearance of high piezoelectric coefficients in some SLs with the polar discontinuity, we analyzed the third-rank tensors  $\partial u_\alpha^i / \partial \sigma_{\mu\nu}$ . This tensor characterizes the displacement of the  $i$ th atom in the unit cell in the  $\alpha$  direction produced by the strain described by the  $\sigma_{\mu\nu}$  tensor. It turned out

TABLE IV. The values of  $\partial u_\alpha^i / \partial \sigma_{15}$  (in Å) of the  $\partial u_\alpha^i / \partial \sigma_{\mu\nu}$  tensors for all atoms in the ground-state  $P4bm$  structure of PbTiO<sub>3</sub>/LaAlO<sub>3</sub> and BaTiO<sub>3</sub>/LaAlO<sub>3</sub> superlattices ( $A = \text{Pb}$  and  $\text{Ba}$ , respectively). Atoms 11–20 are located in the adjacent cell of the doubled unit cell of the high-temperature phase.

Atom $i$	PbTiO <sub>3</sub> /LaAlO <sub>3</sub>	BaTiO <sub>3</sub> /LaAlO <sub>3</sub>
A(1)	+5.18	+0.086
Ti(2)	+2.37	-0.083
O(3)	-1.19	+0.239
O(4)	-5.61	+0.099
O(5)	-1.02	-0.109
La(6)	+4.56	+0.731
Al(7)	+0.76	+0.016
O(8)	-0.21	-0.314
O(9)	-0.22	-0.154
O(10)	-0.84	-0.097
A(11)	+1.71	-0.383
Ti(12)	+2.37	-0.083
O(13)	-1.19	+0.239
O(14)	-5.61	+0.099
O(15)	-1.02	-0.109
La(16)	+0.48	+0.370
Al(17)	+0.76	+0.016
O(18)	-0.21	-0.314
O(19)	-0.22	-0.154
O(20)	-0.84	-0.097

that in superlattices exhibiting the strong piezoelectric response, the values of some components of these tensors for some atoms reach 10–15 Å (that is, a deformation of the unit cell by 1% causes the atomic displacements that exceed 0.1 Å). For example, in the PbTiO<sub>3</sub>/LaAlO<sub>3</sub> SL, such atoms are Pb(1), La(6), and two oxygen O(4) and O(14) atoms located in the TiO<sub>2</sub> layer (Table IV); the

contributions of the O(8) and O(9) oxygen atoms located in the  $\text{AlO}_2$  layer are 25 times smaller. Isolation of such atomic groups and analysis of their local structure may be a way to better understand the microscopic mechanism of the appearance of the strong piezoelectricity and to use this information for intentional modification of materials in order to obtain high piezoelectric properties.

A comparison of the piezoelectric properties of the metastable  $Cc$  phase and the ground-state  $Pc$  phase for  $\text{KNbO}_3/\text{SrTiO}_3$  and  $\text{SrTiO}_3/\text{KTaO}_3$  SLs showed that their piezoelectric tensors are fairly close to each other, with a typical deviation of the piezoelectric coefficients of 4–6%.

According to our calculations, the piezoelectric coefficients in studied SLs can reach 150–270 pC/N. A comparison of the obtained results with the published data finds their reasonable agreement. For the  $P4mm$  phase of the  $\text{PbTiO}_3/\text{LaAlO}_3$  SL, our result  $e_{33} = -3.52 \text{ C/m}^2$  is close to the  $e_{33} = -2.85 \text{ C/m}^2$  value calculated in [28]. However, our  $d_{33} = -18.9 \text{ pC/N}$  value calculated for the same phase of this SL disagrees with the  $d_{33} = +13.9 \text{ pC/N}$  value obtained in [29]. These values are close in magnitude but different in sign. A possible reason for a stronger discrepancy here may be the neglect in [29] of the difference in displacements and effective charges of the oxygen atoms (their effective charge varies from  $-2.07$  to  $-5.84$ ). As for the  $\text{PbTiO}_3/\text{KTaO}_3$  superlattice studied in [40], the values of the  $e_{33}$  and  $e_{15}$  coefficients obtained there are two orders of magnitude lower than our data, and the  $e_{31}$  coefficient is close to our result in magnitude, but differs in sign.

## IV. CONCLUSIONS

Using first-principles calculations, the stability of high-symmetry  $P4mm$  polar phase in eleven ferroelectric perovskite superlattices with the polar discontinuity have been studied. It was shown that in most superlattices, this phase exhibits either the ferroelectric or the antiferrodistortive (AFD), or both of these instabilities simultaneously. In superlattices exhibiting only the ferroelectric instability, the  $Cm$  phase is the ground state. In superlattices exhibiting only the AFD instability, the  $P4bm$  phase is the ground state. And finally, in superlattices in which the  $P4mm$  phase exhibits both the ferroelectric and AFD instabilities, the  $Pc$  phase is the ground state. In superlattices whose structure exhibits the AFD instability, the structure of metastable phases was also calculated. The average spontaneous polarization and piezoelectric properties for the ground-state structures of all superlattices were calculated. It was shown that the appearance of high piezoelectric coefficients is due to the strain-induced local rearrangement of certain atomic groups inside the primitive cell.

## ACKNOWLEDGMENTS

This work was supported by the Russian Foundation for Basic Research (RFBR) under Grant 17-02-01068.

- 
- [1] M. Dawber, K. M. Rabe, and J. F. Scott, Physics of thin-film ferroelectric oxides, *Rev. Mod. Phys.* **77**, 1083 (2005).
  - [2] P. Ghosez and J. Junquera, First-principle modeling of ferroelectric oxide nanostructures, in *Handbook of Theoretical and Computational Nanotechnology*, Vol. 9, edited by M. Rieth and W. Schommers (American Scientific Publishers, 2006) pp. 623–728.
  - [3] D. Bao, Multilayered dielectric/ferroelectric thin films and superlattices, *Curr. Opin. Solid State Mater. Sci.* **12**, 55 (2008).
  - [4] J. Junquera and P. Ghosez, First-principles study of ferroelectric oxide epitaxial thin films and superlattices: Role of the mechanical and electrical boundary conditions, *J. Comput. Theor. Nanosci.* **5**, 2071 (2008).
  - [5] A. I. Lebedev, Ab initio studies of dielectric, piezoelectric, and elastic properties of  $\text{BaTiO}_3/\text{SrTiO}_3$  ferroelectric superlattices, *Phys. Solid State* **51**, 2324 (2009).
  - [6] A. I. Lebedev, Ground state and properties of ferroelectric superlattices based on crystals of the perovskite family, *Phys. Solid State* **52**, 1448 (2010).
  - [7] A. I. Lebedev, Ground-state structure of  $\text{KNbO}_3/\text{KTaO}_3$  superlattices: Array of nearly independent ferroelectrically ordered planes, *Phys. Status Solidi B* **249**, 789 (2012).
  - [8] Y. I. Yuzyuk, Raman scattering spectra of ceramics, films, and superlattices of ferroelectric perovskites: A review, *Phys. Solid State* **54**, 1026 (2012).
  - [9] A. I. Lebedev, Properties of  $\text{BaTiO}_3/\text{BaZrO}_3$  ferroelectric superlattices with competing instabilities, *Phys. Solid State* **55**, 1198 (2013).
  - [10] Y. A. Tikhonov, A. G. Razumnaya, O. A. Maslova, I. N. Zakharchenko, Y. I. Yuzyuk, N. Ortega, A. Kumar, and R. S. Katiyar, Phase transitions in two- and three-component perovskite superlattices, *Phys. Solid State* **57**, 486 (2015).
  - [11] A. Ohtomo and H. Y. Hwang, A high-mobility electron gas at the  $\text{LaAlO}_3/\text{SrTiO}_3$  heterointerface, *Nature* **427**, 423 (2004).
  - [12] A. Brinkman, M. Huijben, M. van Zalk, J. Huijben, U. Zeitler, J. C. Maan, W. G. van der Wiel, G. Rijnders, D. H. A. Blank, and H. Hilgenkamp, Magnetic effects at the interface between non-magnetic oxides, *Nature Mater.* **6**, 493 (2007).
  - [13] N. Reyren, S. Thiel, A. D. Caviglia, L. F. Kourkoutis, G. Hammerl, C. Richter, C. W. Schneider, T. Kopp, A.-S. Rüetschi, D. Jaccard, M. Gabay, D. A. Muller, J.-M. Triscone, and J. Mannhart, Superconducting interfaces between insulating oxides, *Science* **317**, 1196 (2007).
  - [14] A. D. Caviglia, S. Gariglio, N. Reyren, D. Jaccard, T. Schneider, M. Gabay, S. Thiel, G. Hammerl, J. Mannhart, and J.-M. Triscone, Electric field

- control of the  $\text{LaAlO}_3/\text{SrTiO}_3$  interface ground state, *Nature* **456**, 624 (2008).
- [15] K. Yang, S. Nazir, M. Behtash, and J. Cheng, High-throughput design of two-dimensional electron gas systems based on polar/nonpolar perovskite oxide heterostructures, *Sci. Rep.* **6**, 34667 (2016).
- [16] B. Yin, P. Aguado-Puente, S. Qu, and E. Artacho, Two-dimensional electron gas at the  $\text{PbTiO}_3/\text{SrTiO}_3$  interface: An ab initio study, *Phys. Rev. B* **92**, 115406 (2015).
- [17] J. Ruan, X. Qiu, Z. Yuan, D. Ji, P. Wang, A. Li, and D. Wu, Improved memory functions in multiferroic tunnel junctions with a dielectric/ferroelectric composite barrier, *Appl. Phys. Lett.* **107**, 232902 (2015).
- [18] Q. Wu, L. Shen, M. Yang, J. Zhou, J. Chen, and Y. P. Feng, Giant tunneling electroresistance induced by ferroelectrically switchable two-dimensional electron gas at nonpolar  $\text{BaTiO}_3/\text{SrTiO}_3$  interface, *Phys. Rev. B* **94**, 155420 (2016).
- [19] E. Y. Tsymlal and H. Kohlstedt, Tunneling across a ferroelectric, *Science* **313**, 181 (2006).
- [20] J. P. Velev, C.-G. Duan, J. D. Burton, A. Smogunov, M. K. Niranjan, E. Tosatti, S. S. Jaswal, and E. Y. Tsymlal, Magnetic tunnel junctions with ferroelectric barriers: Prediction of four resistance states from first principles, *Nano Lett.* **9**, 427 (2009).
- [21] É. D. Murray and D. Vanderbilt, Theoretical investigation of polarization-compensated II-IV/I-V perovskite superlattices, *Phys. Rev. B* **79**, 100102 (2009).
- [22] M. K. Niranjan, Y. Wang, S. S. Jaswal, and E. Y. Tsymlal, Prediction of a switchable two-dimensional electron gas at ferroelectric oxide interfaces, *Phys. Rev. Lett.* **103**, 016804 (2009).
- [23] N. C. Bristowe, E. Artacho, and P. B. Littlewood, Oxide superlattices with alternating  $p$  and  $n$  interfaces, *Phys. Rev. B* **80**, 045425 (2009).
- [24] Y. Wang, M. K. Niranjan, S. S. Jaswal, and E. Y. Tsymlal, First-principles studies of a two-dimensional electron gas at the interface in ferroelectric oxide heterostructures, *Phys. Rev. B* **80**, 165130 (2009).
- [25] M. Stengel and D. Vanderbilt, Berry-phase theory of polar discontinuities at oxide-oxide interfaces, *Phys. Rev. B* **80**, 241103 (2009).
- [26] H. Das, N. A. Spaldin, U. V. Waghmare, and T. Saha-Dasgupta, Chemical control of polar behavior in bicomponent short-period superlattices, *Phys. Rev. B* **81**, 235112 (2010).
- [27] P. García-Fernández, P. Aguado-Puente, and J. Junquera, Lattice screening of the polar catastrophe and hidden in-plane polarization in  $\text{KNbO}_3/\text{BaTiO}_3$  interfaces, *Phys. Rev. B* **87**, 085305 (2013).
- [28] H. Das, U. V. Waghmare, and T. Saha-Dasgupta, Piezoelectrics by design: A route through short-period perovskite superlattices, *J. Appl. Phys.* **109**, 066107 (2011).
- [29] Z. Zhu, First-principles study of polarization and piezoelectricity behavior in tetragonal  $\text{PbTiO}_3$ -based superlattices, *Chin. Phys. B* **27**, 027701 (2018).
- [30] S.-E. Park and T. R. Shrout, Ultrahigh strain and piezoelectric behavior in relaxor based ferroelectric single crystals, *J. Appl. Phys.* **82**, 1804 (1997).
- [31] R. Guo, L. E. Cross, S.-E. Park, B. Noheda, D. E. Cox, and G. Shirane, Origin of the high piezoelectric response in  $\text{PbZr}_{1-x}\text{Ti}_x\text{O}_3$ , *Phys. Rev. Lett.* **84**, 5423 (2000).
- [32] A. M. Rappe, K. M. Rabe, E. Kaxiras, and J. D. Joannopoulos, Optimized pseudopotentials, *Phys. Rev. B* **41**, 1227 (1990).
- [33] A. I. Lebedev, Ab initio calculations of phonon spectra in  $\text{ATiO}_3$  perovskite crystals ( $A = \text{Ca}, \text{Sr}, \text{Ba}, \text{Ra}, \text{Cd}, \text{Zn}, \text{Mg}, \text{Ge}, \text{Sn}, \text{Pb}$ ), *Phys. Solid State* **51**, 362 (2009).
- [34] A. I. Lebedev, Phase transitions and metastable states in stressed  $\text{SrTiO}_3$  films, *Phys. Solid State* **58**, 300 (2016).
- [35] R. Yu and H. Krakauer, First-principles determination of chain-structure instability in  $\text{KNbO}_3$ , *Phys. Rev. Lett.* **74**, 4067 (1995).
- [36] The numbers of irreducible representations used in this work follow their classification adopted at Bilbao Crystallographic Server [41].
- [37] N. A. Pertsev, A. G. Zembilgotov, and A. K. Tagantsev, Effect of mechanical boundary conditions on phase diagrams of epitaxial ferroelectric thin films, *Phys. Rev. Lett.* **80**, 1988 (1998).
- [38] O. Diéguez, S. Tinte, A. Antons, C. Bungaro, J. B. Neaton, K. M. Rabe, and D. Vanderbilt, Ab initio study of the phase diagram of epitaxial  $\text{BaTiO}_3$ , *Phys. Rev. B* **69**, 212101 (2004).
- [39] The periodicity of a superlattice assumes that the electric field strengths  $E_1$  and  $E_2$  in its layers satisfy the condition  $E_1x_1 + E_2x_2 = 0$ , where  $x_1$  and  $x_2$  are the thicknesses of individual layers. This condition combined with the equation  $(P_1 + \epsilon_1E_1) - (P_2 + \epsilon_2E_2) = \Delta P$ , in which  $P_1$ ,  $P_2$ ,  $\epsilon_1$ , and  $\epsilon_2$  are the spontaneous polarizations and dielectric constants in two layers, gives a solution to this problem in the linear approximation.
- [40] Z.-Y. Zhu, S.-Q. Wang, and Y.-M. Fu, First-principles study of properties of strained  $\text{PbTiO}_3/\text{KTaO}_3$  superlattice, *Chin. Phys. Lett.* **33**, 026302 (2016).
- [41] Bilbao crystallographic server, <http://www.cryst.ehu.es/>.